JOURNAL OF MATERIALS SCIENCE 19 (1984) 2894–2908

The effects of amorphous phase separation on crystal nucleation kinetics in $BaO–SiO_2$ glasses

Part 2 *Isothermal heat treatments at 700°C*

A. H. RAMSDEN, P. F. JAMES
Department of Ceramics, Glasses and Polymers, University of Sheffield, Sheffield S10 2TZ, UK

The nucleation kinetics of the barium disilicate crystal phase were determined in $BaO–SiO_2$ glasses containing 25.3, 28.5 and 30.4 mol % BaO at 700° C. In the 25.3 and 28.5 glasses, which exhibited amorphous phase separation, marked differences in crystal nucleation occurred in each glass at 700° C, depending on the previous heat treatment, for example whether the glass had been heated at a higher temperature to induce phase separation or whether it had been quenched to suppress phase separation. Moreover, at 700° C phase separation and crystal nucleation occurred simultaneously over an extended period and an increase in crystal nucleation rate with time was observed. This was reflected in curved plots of N_V (number of crystals per unit volume) against time. In contrast, for glass 30.4, which did not phase separate, the plots were linear. The results in glasses 25.3 and 28.5 could be completely explained by changes in composition of the baria-rich amorphous phase. Crystal nucleation rates rose with increase in baria content, i.e. as the composition became closer to $BaO·2SiO_2$. Prior heat treatments produced major shifts in composition of the phases. Also, at 700° C the average baria content of the baria-rich phase increased gradually towards the equilibrium value given by the immiscibility boundary.

1. Introduction

In Part 1 of this paper [1] the internal (volume) nucleation kinetics of the barium disilicate crystal phase were studied in a series of $BaO–SiO_2$ glasses with compositions ranging from 25.3 to 33.1 mol% BaO. For each glass a constant nucleation time of 1 h was used at a series of temperatures from 673 to 807° C. The highest nucleation rates were observed in the 33.1 mol% BaO glass, close to the stoichiometric $BaO·2SiO_2$ composition, and just outside the immiscibility region. Much lower rates were found in the glasses with lower BaO contents including those exhibiting amorphous phase separation. However, it was deduced that phase separation had a marked but indirect effect on crystal nucleation due to the accompanying shift in composition of the baria-rich phase in which crystal nucleation occurred, so that after phase separation at a given temperature the crystal nucleation rates of different glasses tended to converge to similar values. There was no evidence for a significant enhancement of crystal nucleation at the interfaces between the amorphous phases.

In Part 2 the effects of phase separation have been explored in greater detail with three of the glasses in order to test further the ideas developed in Part 1. The crystal nucleation kinetics were determined as a function of time in isothermal heat treatments at 700° C and the morphology of phase separation studied simultaneously by replica electron microscopy . Prior to the nucleation treatment at 700° C some samples of each glass were given heat treatments at higher temperatures (where no internal crystal nucleation occurred) to

0022–2461/84 $03.00 + .12

induce phase separation, and some samples were given no such preliminary treatment. The effects of the phase separation produced by the prior heat treatment on crystal nucleation at 700° C were then determined for each glass separately. This procedure had the advantage of inherent simplicity since the effects of phase separation could be evaluated on a single composition. Furthermore the necessity of comparing different glasses (as in Part 1), with the possibility of complicating effects from small variations in the impurity levels (such as Al_2O_3 or SrO), was avoided.

2. Experimental procedure

Three $BaO–SiO_2$ glasses containing 25.3, 28.5 and 30.4 mol% BaO (glasses B1, B3 and B5 respectively in Part 1) were studied. Glasses B1 and B3 developed amorphous phase separation after suitable heat treatment. No phase separation could be produced in glass B5 (Part 1). The preparation and detailed chemical analysis of these glasses were described in Part 1. Some observations of amorphous phase separation were also discussed. The measured immiscibility temperatures of B1 and B3 were 1140 and 905° C, respectively. Cast rods of B1 showed slight visible opalescence due to fine scale phase separation which had occurred during cooling. Quenched discs of B1 (pressed between steel plates) were visibly clear but EM replicas revealed extremely fine scale phase separation. Cast rods and pressed discs of B3 were visibly clear and fine scale phase separation was not detected on EM replicas (Part 1).

2.1. Crystal nucleation measurements

Small samples (approximately 5 mm x 5 mm x 3 mm in size) were cut from the pressed discs or cast rods of the glasses. Some samples were given various preliminary heat treatments to induce phase separation, as will be described below. All the samples were then heated at the crystal nucleation temperature (700° C) for times from 0.5 to 17 h (B1 and B5) or from 2 to 60 h (B3). The temperature 700° C was selected for two reasons. First, the maximum nucleation rate for all the glasses occurred at approximately this temperature. This enabled greater accuracy of N_V (number of crystals per unit volume) measurements to be obtained since negligible nucleation occurred during heating or cooling compared with the nucleation produced at 700° C. Secondly, amorphous phase separation developed slowly at this temperature so that its effects on crystal nucleation could be followed over an extended period. The quantitative method of determining N_V using optical microscopy was fully described in Part 1. A growth (nuclei development) temperature of 840° C was again employed.

Control samples were used to determine the crystal nucleation densities (N_V) present after the various prior heat treatments, to be described. These samples were also given a development treatment at 840° C. In all cases nucleation in the controls was negligible compared with the nucleation produced by the main treatment at 700° C (between 10 and 10^5 times lower in the controls depending on the nucleation time used at 700° C).

2.2. Heat treatments and thermal histories prior to the crystal nucleation treatment at 700° C

2.2.1. Glass 25.3 (B1)

2.2.1.1. Treatment A. To remove amorphous phase separation as far as possible samples cut from the pressed (rapidly cooled) discs were inserted in a furnace at 1250° C, held at approximately this temperature for one minute, and immediately quenched into silicone oil at room temperature. 1250° C was well above the immiscibility temperature for the glass so that phase separation rapidly redissolved at this temperature. Negligible internal crystal nucleation occurred with this treatment. Some surface crystal nucleation and growth did take place but this was removed at the grinding and polishing stage before examination by optical microscopy.

2.2.1.2. Treatment B. Samples of glass 25.3 were cut from the as-prepared quenched (pressed) glass discs.

2.2.1.3. Treatment C. Samples of the as-prepared glass 25.3 (i.e. Treatment B) were heated at 800° C for 1 h and cooled quickly to room temperature in air. Phase separation occurred rapidly at 800° C and was well developed after 1 h (see the later results in Part 3). Some internal crystal nucleation occurred during this treatment since 800° C is just within the upper range of the nucleation versus temperature curve (see Part 1). This nucleation was found to be negligible compared with that occurring subsequently in the main nucleation treatment at 700° C.

2.2.1.4. Treatment D. Samples of the as-prepared glass 25.3 (treatment B) were heated at 900° C for 10 min and then cooled quickly to room temperature in air. Phase separation also occurred rapidly at 900° C. This treatment was designed to produce a coarser phase separation microstructure than that developed in Treatment C. Again, crystal nucleation occurring during this treatment was negligible compared with the nucleation produced in the main treatment at 700° C.

The heat treatment temperatures used are shown in Fig. 1. It is evident that the equilibrium composition of the BaO-rich matrix phase in glass 25.3 is richer in BaO the lower the heat treatment temperature.

2.2.2. Glass 28.5 (B3)

2.2.2.1. Treatment E. Samples of glass 28.5 were cut from the as-cast glass rods (cooled in air) or from the pressed discs. No phase separation was detected by TEM replicas. No very rapid quenching technique to suppress phase separation (as treatment A above) was required for this glass.

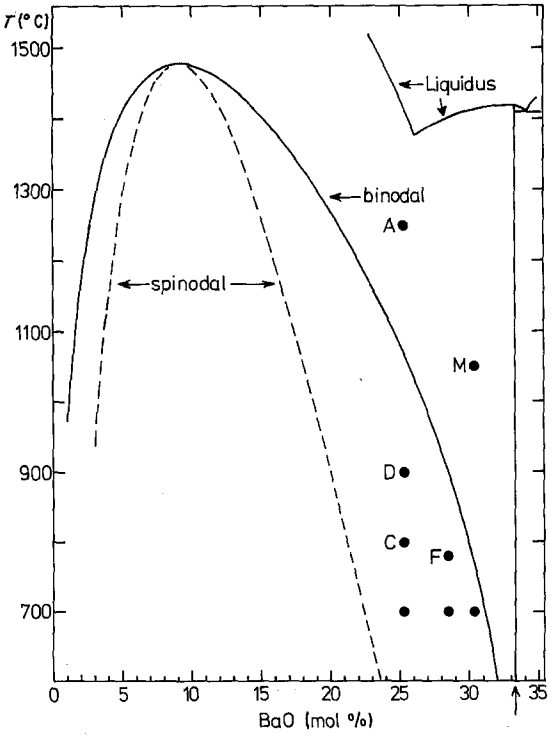

Figure 1 Part of the $BaO-SiO_2$ phase diagram. Immiscibility boundary (binodal) and spinodal curve from [7]. Compositions and heat treatment temperatures used are shown by points (•). $BaO \cdot 2SiO_2$ composition indicated by ↑. See text for full explanation of heat treatments.

2.2.2.2. Treatment F. Samples of the as-prepared glass 28.5 (i.e. Treatment E) were heat treated at 780° C for 1 h to produce well-developed phase separation and cooled quickly to room temperature in air. Some internal crystal nucleation occurred during this treatment as in Treatment C above. Again it was negligible compared with the nucleation produced in the main treatment at 700° C.

The compositions of glasses 28.5 and 25.3 are shown in Fig. 1.

The samples of glass 25.3 given the Treatments A to D will be conveniently referred to as glasses 25.3A to 25.3D or, for brevity, glasses A to D. Similarly the samples of glass 28.5 will be referred to as glasses 28.5E and 28.5F or glasses E and F.

After these prior heat treatments all the samples were nucleated at 700° C for a series of times and developed at 840° C, as described above.

2.3. Amorphous phase separation measurements

Surface carbon replicas of the glasses were prepared for electron microscopy, as described in Part 1 [1], so that stereological data of the phase separation microstructures could be obtained. For this purpose a set of glass samples were given identical heat treatments to the samples used for the crystal nucleation measurements, except that after heat treatment at 700° C no further development treatment at 840° C was employed. Parameters characterizing the phase morphologies were determined from enlarged prints of the micrographs. The interfacial area of the dispersed (silica-rich) phase per unit volume, S_v, was obtained by drawing random lines on the prints and counting the number of intersections per unit length (N_L) with the phase boundaries. S_v was given by $2N_L$ [2, 3]. For microstructures consisting of isolated droplets, the numbers of droplets per unit volume, n_v, were determined by essentially the same method as used to measure N_v for the crystal spherulites in the optical micrographs (see Part 1). Some values of the area fraction of the dispersed phase, which ideally is equal to the volume fraction V_f, were also obtained by the standard point counting technique [2].

The systematic errors inherent in the replica technique were studied by Burnett and Douglas [4]. Over etching of the glass surface may lead to a large overestimate of V_f, the volume fraction of dispersed phase. Burnett and Douglas were able to

improve the accuracy by plotting apparent V_f against etching time and extrapolating back to zero time. Unfortunately, this was impractical for the present glasses since the very fine microstructures were not adequately revealed if the etching treatment (with dilute HF) was very light.

Absolute errors due to over etching were shown to occur since measured V_f values for the present glasses [5] were typically 25% higher than the theoretical (calculated) values from the published immiscibility boundary [6, 7], the known glass compositions and densities. Similarly, the absolute values of S_v and n_v were probably overestimated. However, an identical etching treatment was used for all the glasses. Thus the measurements provided valuable quantitative comparisons between the glasses and approximate, but useful, infomation on the development of phase separation in the various compositions. From a purely statistical viewpoint the 95% confidence limits in the measured values of S_v and n_v were ±10% of the mean values.

3. Results and discussion

3.1. Amorphous phase separation in glass 25.3 (B1)

Representative micrographs illustrating the phase morphologies in glass 25.3 given the various heat treatments (A to D) described above are shown in Fig. 2. The stereological measurements are given in Table I. There were marked differences between the various treatments. The as-prepared glass B contained a high density of very fine droplets (average diameter 20 to 30 nm). With heat treatment at 700° C changes were observed on the replicas. After several hours the average droplet diameter increased to approximately 40 nm. Also the structure appeared to become more interconnected making the number of droplets (n_v) difficult to determine accurately. Whereas the n_v showed little change (Table I), the interfacial area, S_v, showed a small increase. No phase separation was detected in the very rapidly quenched glass A (Fig. 2). However, a high density of very fine droplets was detected after several hours at 700° C. Subsequently, the changes were similar to glass B and no measurements were attempted.

The phase separation in glasses C and D was coarser than in glasses A and B (Fig. 2). The average droplet diameters for C and D were approximately 45 and 85 nm, respectively. The S_v and n_v values of glasses C and D were correspondingly smaller than those of glass B. After heat treatment at 700° C the already phase-separated glass D showed little evidence of any changes, in contrast to glasses A and B. The n_v and S_v values for glass D remained constant. However, in glass C S_v did show a significant increase with time of heat treatment.

Previous studies of phase separation at a constant temperature [4, 8] have shown that n_v, S_v and V_f initially increase with time if the early stage is governed by nucleation and growth. Eventually V_f approaches a constant value. At about the same stage coarsening (Ostwald ripening) begins to predominate so that n_v and S_v reach a maximum and then decrease. Previous studies [8] have also shown that a glass phase-separated at a higher temperature may undergo secondary phase separation at a lower temperature. This occurs because one of the phases itself can phase separate on cooling to the second (lower) temperature. The matrix between the larger droplets present after the first stage heat treatment may thus separate into many fine droplets. Alternatively, the larger droplets may simply grow,

TABLE I S_v ($m^2 m^{-3}$) $\times 10^{-7}$ and n_v (m^{-3}) $\times 10^{-20}$ for glasses 25.3B, 25.3C and 25.3D (see text) after heat treatment at 700° C

Time of heat treatment (h)	Glass 25.3B		Glass 25.3C		Glass 25.3D	
	S_v	n_v	S_v	n_v	S_v	n_v
0	4.1	100	3.0	–	2.0	–
1	4.5	100	3.6	49	2.0	–
2	5.3	90	3.7 (2.1 h)	50 (2.1 h)	2.0	8.2
4	5.0	–	3.7 (4.2 h)		–	–
7.58	–	–	–		1.9	8.2
8.7	5.0	–	–		–	
11.42	–	–	–		2.0	
12.25	–	–	4.2			
16.62	5.0	92				

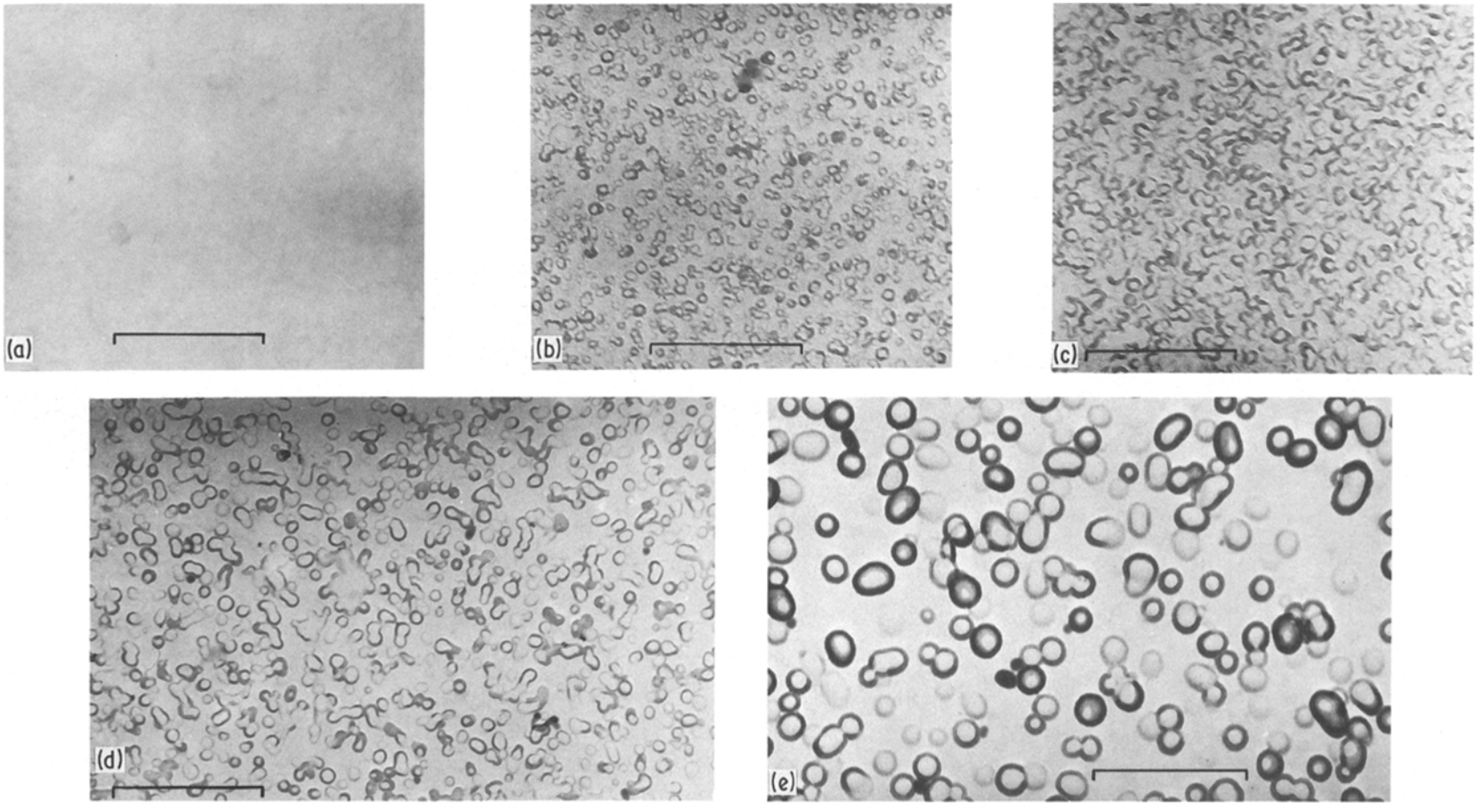

Figure 2 Replica electron micrographs (75 kV) of glass 25.3. (a) Rapidly quenched glass (Treatment A); (b) as-prepared glass (Treatment B) heated at 700° C for 1 h; (c) as-prepared glass (B) heated at 700° C for 8 h; (d) glass heat treated at 800° C for 1 h (Treatment C) followed by 700° C for 2.1 h; (e) glass heat treated at 900° C for 10 min (Treatment D) followed by 700° C for 1 h. The bars denote 0.5 μm.

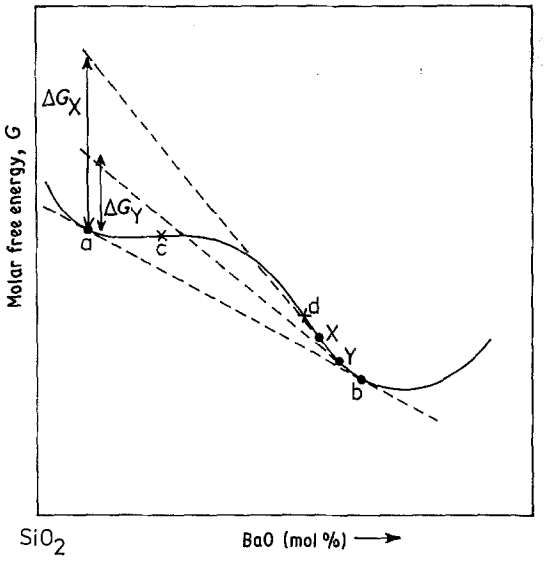

Figure 3 Schematic free energy against composition diagram for $BaO-SiO_2$ system illustrating thermodynamic driving force, ΔG [1, 8] for separation of silica-rich amorphous phase at 700° C. ΔG_X represents driving force for primary separation in an initially homogeneous glass X (e.g. glass 25.3 A). ΔG_Y represents driving force for secondary phase separation in the matrix phase Y of the glass after a prior phase separation treat treatment at a higher temperature (e.g. glasses 25.3C or 25.3D). Equilibrium phase compositions are a and b, spinodal compositions are c and d.

with no additional precipitation of fine droplets.

From the immiscibility curve for $BaO-SiO_2$ [6, 7] the baria-rich phases at 700, 800 and 900° C contain 31.1, 30.0 and 28.5 mol. % BaO, respectively. The latter two figures correspond to the baria-rich matrix phases in glasses C and D, respectively. The thermodynamic driving force for nucleation of droplets was greatest in glasses A and B (see Fig. 3). This accounted for the fine scale phase separation occurring in glass B during quenching and in glass A during heat treatment at 700° C. There was evidence from the replicas for a further gradual phase separation in glass B at 700° C by the growth of the existing fine droplets. The driving forces for secondary nucleation of droplets in the baria-rich matrix phases of glasses C and D were lower than the driving forces for primary nucleation of droplets in glasses A or B. In fact no secondary nucleation in glasses C and D was observed at 700° C. Evidence that additional phase separation occurred in glasses C and D as well as in glasses A and B probably by the growth

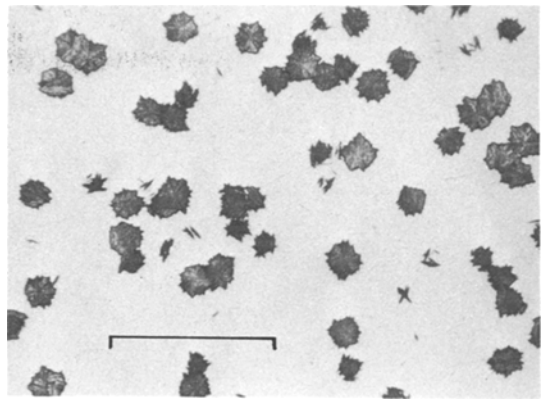

Figure 4 Typical reflection optical micrograph of polished and lightly etched section of glass 25.3B showing crystal spherulites of barium disilicate. Glass 25.3B given nucleation treatment 700° C for 2.1 h followed by a short growth (development) treatment at 840° C. The bar denotes 50 μm.

of the existing droplets, will shortly be presented from the crystal nucleation study.

3.2. Crystal nucleation in glass 25.3

Fig. 4 is a typical optical micrograph used to determine N_v in glass 25.3 given one of the prior head treatments (A to D) followed by crystal nucleation at 700° C and growth at 840° C. Marked differences in crystal nucleation behaviour were observed between the specimens with different initial heat treatments. The N_v values are given in Table II and are plotted against time in Figs. 5a to c. For clarity the earlier stages are plotted separately.

The nucleation rates (I) are plotted against time in Fig. 5d. These were obtained from the slopes of the N_v against time plots, but the method used requires brief discussion. The first two I values for glasses A, B and D (at 0.75 and 1.55 h) were calculated from two adjacent points on the N_v plots due to the large curvatures observed at early times on these plots. The other I values for A, B and D were the slopes of "best" (least-squares) straight lines fitted to groups of three successive points along the N_v against time curves. For glass C the I values in Fig. 5d were obtained in the same way from groups of four successive points on the N_v against time curves. The choice of the appropriate number of points (here 2, 3 or 4) depended upon the degree of curvature of the N_v against time plots involved. The nucleation rates in Fig. 5d are approximate only but are useful as an indication of the general trends over a long period of

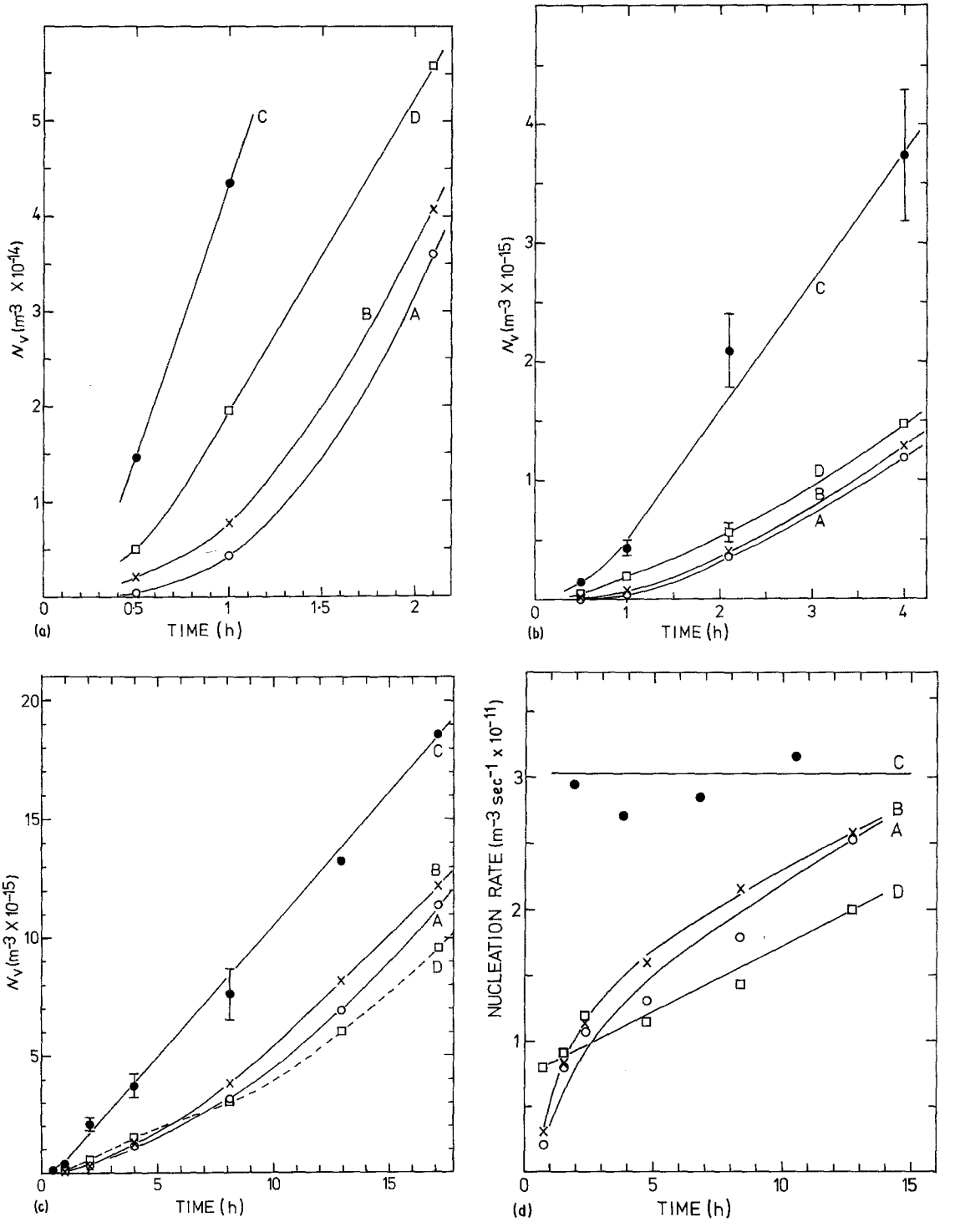

Figure 5 (a) to (c) Crystal nucleation kinetics in glass 25.3 at 700° C. N_V against time plots (N_V is the number of internally nucleated spherulites of crystalline barium disilicate per unit volume) after prior heat treatments A, B, C and D (see text). Early stages shown in (a) and (b) and later stages in (c). Points ○ (A), × (B), • (C) and □ (D). 95% confidence limits ±15% of values (marked ⊢——⊣). In (c) a "least-squares" straight line is fitted to the values for glass C.

(d) Crystal nucleation rates against time for glasses 25.3A, B, C and D determined from N_V against time plots in Figs. 5a to c. using method described in text. Points ○ (A), × (B), • (C) and □ (D). Line for glass 25.3C is average nucleation rate from least-squares fit to all points on N_V against time plot.

TABLE II Crystal nucleation data for glasses 25.3A, B, C. D (see text) after heat treatment at 700° C (95% confidence limits are ±15% of N_v value)

Time of heat treatment (h)	$N_v \times 10^{-12}$ (m^{-3})			
	25.3A	25.3B	25.3C	25.3D
0.5	4.77	21.9	147	51.3
1	43.0	78.0	434	196
2.1	361	407	2090	558
4	1190	1290	3730	1470
8.12	3180	3830	7600	3070
12.92	6920	8180	1.32×10^4	6050
17.12	1.14×10^4	1.22×10^4	1.86×10^4	9590

time. The nucleation rates are characteristic of the glass at a particular time whilst the cumulative number of nuclei (N_v) depends on the conditions previously existing in the glass.

The differences between glasses A to D were more marked at the earlier times. The N_v plots of A, B and D exhibited noticeable curvature. The plot for glass C also appeared slightly curved but a straight line could be drawn through the points for longer times to within experimental error. Glass C had consistently higher N_v values than the other glasses. The curves of A and B are very similar, with the curve for B always slightly above that of A. This testified to the accuracy of the method of determining N_v because a small difference was maintained consistently over a long period of time. After about 6 to 7 h the curves for A and B crossed that of D. At shorter times D had a higher value of N_v than A or B. At longer times the reverse applied.

The differences between the glasses became less pronounced at longer times. After 17 h (Fig. 5c) the nucleation rates in all the glasses were steadily approaching the same value.

It will be shown that all the crystal nucleation behaviour can be explained in terms of differences in the composition of the continuous baria-rich matrix phase for the various glasses, and changes in this composition with time. In [1] it was established that the highest crystal nucleation rates at all temperatures occurred in a glass of the stoichiometric barium disilicate composition, and that the nucleation rates decreased with an increase in the silica content of the glass.

The main features in Fig. 5 are readily explained. The higher N_v values and higher nucleation rates in glass C arose from the extensive degree of phase separation initially present in this glass due to the treatment at 800° C. At this stage the baria-rich matrix contained 30.0 mol% BaO (assuming it had reached equilibrium). After heat treatment at 700° C the matrix gradually approached 31.1 mol% BaO. The results indicated that the matrix phase in C, for all times at 700° C, had the highest BaO content (i.e. it was closest to the barium disilicate composition throughout). The higher N_v and nucleation rate values in glass D compared with glasses A and B for the early times at 700° C were also due to the phase separation treatment at 900° C. In this case the BaO content of the matrix phase was probably initially about 28.5 mol% (assuming again attainment of equilibrium, see Section 3.1).

The curvature of the plots of N_v against time may be attributed to phase separation occurring in the glasses simultaneously with the crystal nucleation. The effect is very noticeable in glasses A and B, particularly at shorter times. In these glasses phase separation occurred at 700° C over an extended period of time during which the matrix phase became progressively richer in baria, approaching the equilibrium 31.1 mol% BaO composition. Consequently the crystal nucleation rate steadily increased with time. The curvature of the plot for glass D indicates that additional (secondary) phase separation occurred at 700° C in this glass causing a similar composition shift. As mentioned above, the N_v plot for glass C could be represented as a straight line to within experimental error. However, a noticeable curvature could be discerned for times greater than 4 h, suggesting that secondary phase separation was also taking place in this glass at 700° C. This interpretation for glass C is tentative but is supported by the replica results (Section 3.1).

The quenched (pressed) glass B showed a high density of very fine silica-rich droplets. However, the average baria content of the matrix phase in B was probably much lower than in the glasses C and D (somewhat greater than 25.3 mol% BaO

but less than 28.5 mol% BaO, the matrix composition in D). Thus for the early times at 700° C the crystal nucleation rate in B was less than in glasses C and D. Phase separation occurred in all the glasses at 700° C. However, the greater thermodynamic driving force (Fig. 3) for composition B caused faster nucleation and growth of silica-rich droplets in this glass than in glasses C or D. Also the larger number of fine droplets already present in B provided many more sites for diffusion controlled growth than in C and D, again causing faster precipitation of the silica-rich phase. Consequently the composition of the matrix phase in B changed more rapidly in glass B than in glasses C or D. Eventually the matrix composition in B became richer in baria than the matrix composition in D. Thus the crystal nucleation rates for B and D coincided after about 2 h and thereafter were greater in glass B (Fig. 5). Also, a cross-over in the N_v against time plot occurred with B overtaking D at about 6 h.

Very similar arguments to the proceding may be applied to glass A. The somewhat lower N_v values in A compared with B, particularly for early times at 700° C, were due to the severe initial quenching treatment given to A, which suppressed phase separation. On heating at 700° C fine scale separation appeared and composition changes in the matrix phase occurred producing a N_v against time plot similar to that of glass B.

Let us consider the possibility of explaining the above results in terms of crystal nucleation catalysed at the interfaces between the amorphous phases. The various possible mechanisms associated with the interfaces were discussed in Part 1 [1]. If such mechanisms were operative the interfacial area S_v of phase separation would be of crucial importance. If the phase morphology resembled isolated droplets then the number of droplets n_v would also be important because two or more crystals nucleating around a droplet would eventually coalesce and be recorded as one crystal. Thus each droplet would give rise to only one crystal, regardless of droplet size.

It is clear from the results that an "interface" mechanism does not provide a satisfactory alternative to the "composition" mechanism discussed previously. For example, glass B had a larger S_v than glass C, yet B had the lower crystal nucleation rates. This is opposite to the result expected if crystal nucleation occurred predominantly at interfaces. Furthermore, glass B contained ten times more droplets than glass D and more droplets than glass C. However, for the early times at 700° C the crystal nucleation rate of glass B was less than (or similar to) that of glass D and much smaller than that of glass C. There is therefore no evidence for enhancement of crystal nucleation at the interfaces from these results.

3.3. Subsidiary crystal nucleation experiments on glass 30.4

A possible explanation of the curvatures of the N_v against time plots is that they are caused by transient (non-steady state) nucleation, independent of the effects of phase separation. In this process the steady state (constant) crystal nucleation rate in a supercooled liquid at constant temperature is not achieved immediately, but only after the elapse of a certain induction time. A period of time is required to create a steady state size distribution of crystal embryos in the liquid. Non-steady state nucleation has been studied in non phase-separating glasses [9]. It is only important at lower temperatures and is characterized by a curved N_v against time plot, becoming linear at longer times with a positive intercept on the time axis. At higher temperatures, where transient effects disappear the N_v against time plots are linear and pass through the origin.

To see if transient nucleation could be important in glass 25.3 at 700° C, a glass which did not phase separate, glass 30.4 (B5), was also studied at the same temperature (Table IIIa). The N_v against time plot (Fig. 6) was a straight line passing through the origin to within experimental error. There was no sign of transient effects. However, when the nucleation temperature was lowered to 677° C a marked induction time effect did appear in glass 30.4 (Fig. 6 and Table IIIb),

TABLE IIIa Crystal nucleation data for glasses 30.4 M and 30.4 N (see text) after heat treatment at 700° C. Glass 30.4 N was glass 30.4 as-cast (cooled in air). Glass 30.4 M was glass 30.4 heated at 1050° C for 1 min and rapidly quenched into silicone oil.

Time of heat treatment (h)	$N_v \times 10^{-12}$ (m^{-3})	
	30.4 N	30.4 M
1	383	408
2	1280	1350
4.5	2480	2710
7.75	4370	3960
16.25	9040	8020

TABLE IIIb Crystal nucleation data for glass 30.4 at 677° C

Time of heat treatment (h)	$N_V \times 10^{-12}$ (m^{-3})
1	4.78
2	49.6
4	259
8	2350
16	9200

probably due to the lower diffusion rates at 677° C. The results at 700° C for glass 30.4 indicate that the induction time in glass 25.3 is likely to be small at 700° C. Any curvature on the plots produced by transient effects would occur only at short times (probably for one hour at most). The steady curvatures observed for times up to 16 h were therefore caused by phase separation within the glasses.

The experiment described above on glass 30.4 at 700° C was also carried out to check the possibility that thermal history (in this case quenching rate) might in some way influence the crystal nucleation behaviour even in a glass which did not exhibit phase separation. Some samples of glass 30.4 were obtained from as-cast rods cooled in air ("glass 30.4 N"). Samples were also placed in a furnace at 1050° C, held at this temprature for about 1 min and rapidly quenched into silicone oil at room temperature ("glass 30.4 M"). This was intended to be comparable to the treatment A given to glass 25.3 discussed earlier. The samples were subsequently nucleated at 700° C in the normal way. No significant difference in nucleation behaviour between the two sets of samples was observed, the results agreeing to within the 95% confidence limits (Table IIIa, Fig. 6).

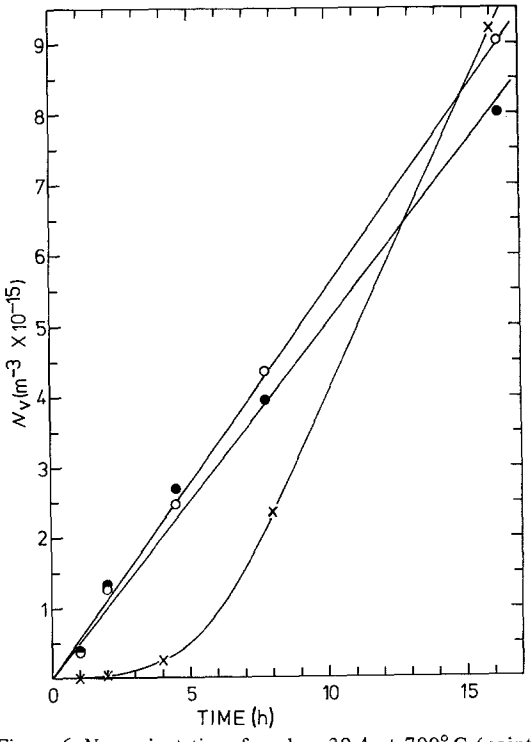

Figure 6 N_V against time for glass 30.4 at 700° C (points ○ and ●) and at 677° C (points X). Points ○ are for as-cast glass (30.4N) and points ● are for rapidly quenched glass (30.4M). Least-squares fits to data at 700° C are shown.

3.4. Amorphous phase separation in glass 28.5 (B3)

Representative micrographs illustrating the phase morphologies in glass 28.5 given the heat treatments (E and F) described above are shown in Fig. 7. The stereological measurements are displayed in Table IV. This glass had a lower immiscibility temperature than glass 25.3. As a result it phase separated less easily and produced a more "droplet-like" and less interconnected microstructure. No phase separation was detected by EM replicas in the rapidly air cooled glass E (Fig. 7) or in glass E heated for 2 h at 700° C. After 6 h at 700° C a large number of fine droplets (diameters approximately 10 nm) were clearly visible. After 21 h at 700° C the average particle diameter had increased to approximately 25 nm. Thus phase separation developed in glass E in the first few hours of heat treatment at 700° C. As mentioned earlier, the values of S_V and n_V were approximate but were useful for comparative purposes. Both S_V and n_V increased in the early stages and showed peaks at about 13 h at 700° C (Table IV). This indicates that the coarsening process (Ostwald ripening) began to predominate over the early stage nucleation and growth of droplets after about 13 h in glass E (see also Section 3.1).

Glass F (glass 28.5 given a prior heat treatment at 780° C for 1 h) showed much coarser phase separation than glass E. The average droplet diameter was approximately 50 nm. The additional heat treatment at 700° C had little obvious effect on the appearance of the phase separation microstructure. Also the S_V and n_V values remained virtually constant apart from a small and possible significant increase, from 2 to 6 h.

It is clear that primary phase separation occurred in glass E at 700° C. Following similar arguments to those used for glass 25.3 (Section 3.1

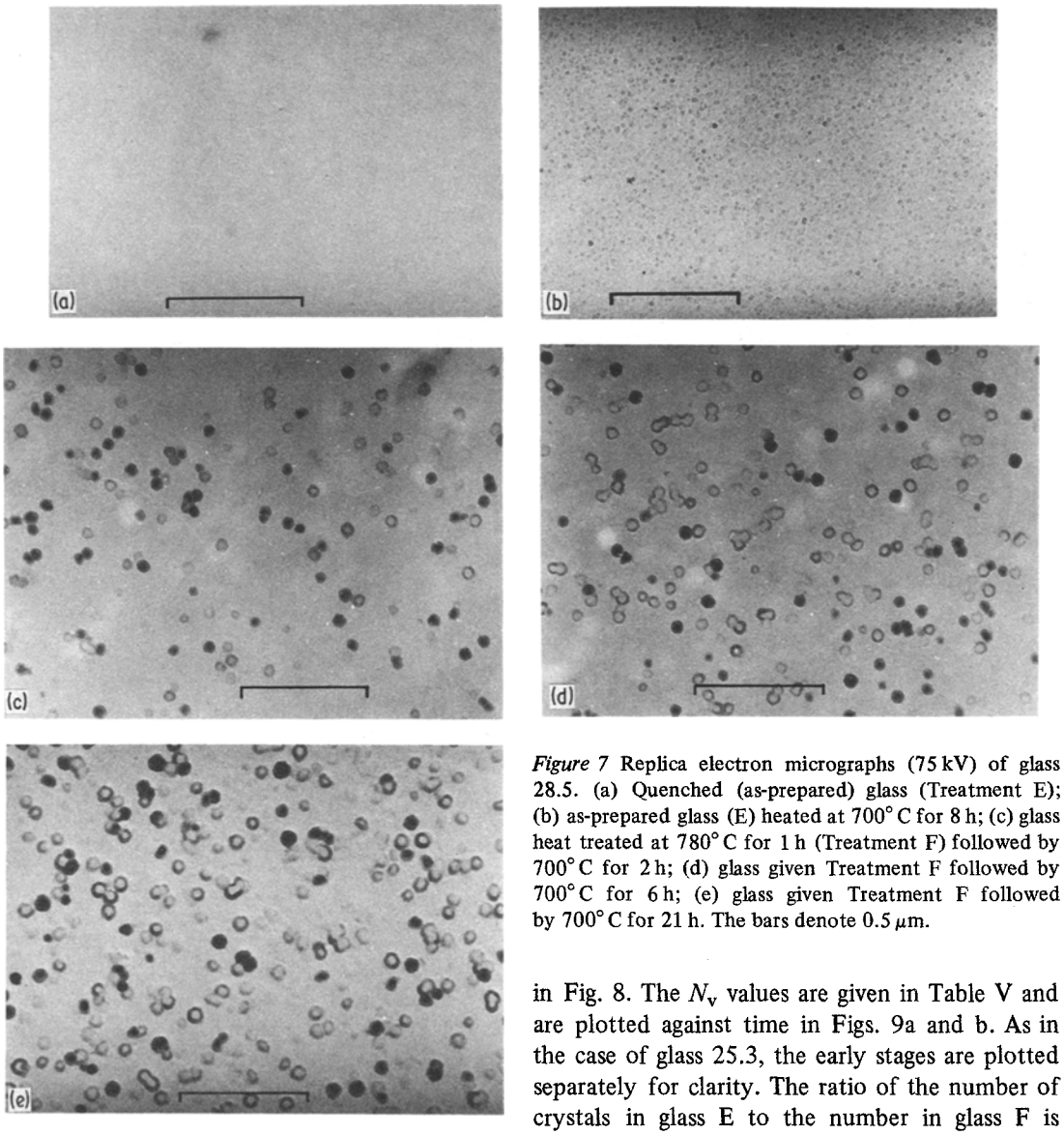

Figure 7 Replica electron micrographs (75 kV) of glass 28.5. (a) Quenched (as-prepared) glass (Treatment E); (b) as-prepared glass (E) heated at 700° C for 8 h; (c) glass heat treated at 780° C for 1 h (Treatment F) followed by 700° C for 2 h; (d) glass given Treatment F followed by 700° C for 6 h; (e) glass given Treatment F followed by 700° C for 21 h. The bars denote 0.5 μm.

and Fig. 3) the thermodynamic driving force for nucleation of droplets was greater in glass E than in glass F, since the matrix phase in glass F was richer in baria than the initially homogeneous glass E. This explains the much larger number of droplets nucleated in E at 700° C. In glass F secondary phase separation at 700° C probably involved a slow growth of the droplets produced by the prior heat treatment at 780° C and possibly some additional nucleation of fresh droplets.

3.5. Crystal nucleation in glass 28.5

Typical optical micrographs of glasses E and F nucleated at 700° C and grown at 840° C are shown in Fig. 8. The N_v values are given in Table V and are plotted against time in Figs. 9a and b. As in the case of glass 25.3, the early stages are plotted separately for clarity. The ratio of the number of crystals in glass E to the number in glass F is plotted against time in Fig. 9c, and the nucleation rates are shown in Fig. 9d. The nucleation rates were determined by the method used above for

TABLE IV S_v ($m^2 m^{-3}$) $\times 10^{-7}$ and n_v (m^{-3}) $\times 10^{-20}$ for glasses 28.5 E and 28.5 F (see Text) after heat treatment at 700° C

Time of heat treatment (h)	Glass 28.5 E		Glass 28.5 F	
	S_v	n_v	S_v	n_v
2	–	–	0.91	7.2
6	1.8	150	1.3	13
8	3.7	240	–	–
13	8.2	330	1.8	16
17	7.7	190	–	–
21	7.3	190	1.5	16
28	7.4	210		

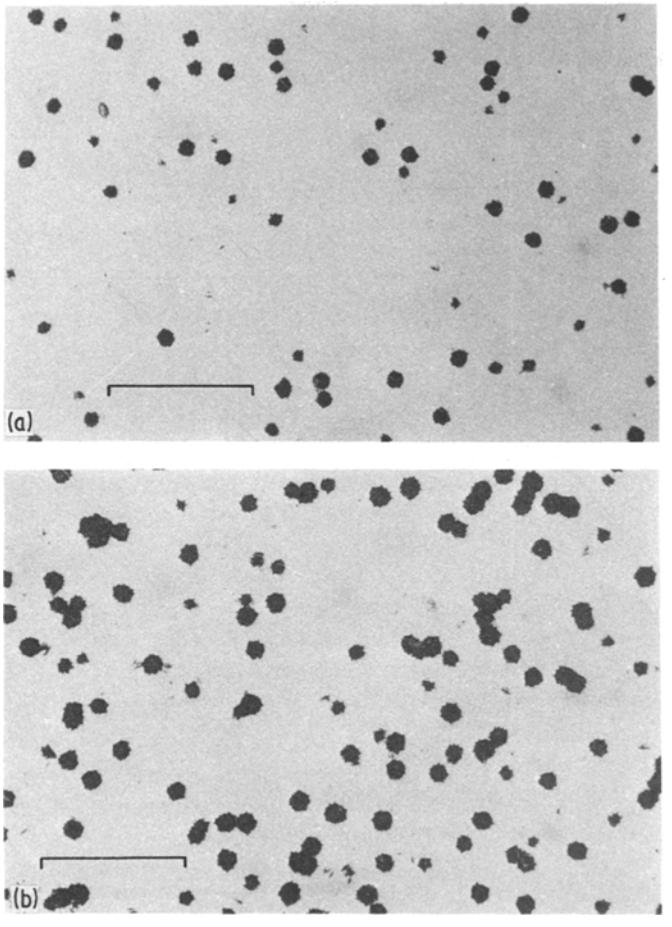

Figure 8 Typical reflection optical micrographs of glass 28.5 showing crystal spherulites of barium disilicate. (a) Glass 28.5E and (b) glass 28.5F. Both glasses E and F given nucleation treatment at 700° C for 1 h followed by a short growth treatment at 840° C. The bars denote 100 μm.

glass 25.3 (Fig. 5d). They were the slopes of "best" (least-squares) straight lines fitted to groups of four successive points along the N_v against time curves.

The prior heat treatment had a marked effect on crystal nucleation at 700° C. The general behaviour is similar to that observed in glass 25.3. For example, there is a curved portion in the N_v against time plots for both E and F. Both curved portions are followed by straight line portions. Again, the curvature can be related to phase separation occurring within the glass during heat treatment at 700° C. At short times the N_v values in glass F were significantly greater than in glass E. For example, the numbers of crystals nucleated in E at times of eight hours or less were consistently about 30 to 40% lower than in F (Figs. 9a and c). Since the 95% confidence limits were ±15% of the mean values, these differences between E and F were significant. Also, the nucleation rates were initially greater in glass F. However, a reversal occurred after about 8 h when the as-poured glass E showed a higher nucleation rate. The N_v values also showed a reversal after about 14 h. Thereafter the N_v values were greater in glass E. Although the individual values for E and F after 14 h were the same to within the 95% confidence limits (±15% of mean values) the "cross-over" is probably significant since the small systematic

TABLE V Crystal nucleation data for glasses 28.5 E and 28.5 F (see text) after heat treatment at 700° C

Time of heat treatment (h)	$N_v \times 10^{-12}$ (m^{-3})	
	28.5 E	28.5 F
2	124	199
4	389	650
6	598	895
8	885	1400
10.53	1380	1650
13	1990	2030
17	3190	3050
21	4110	3640
28.27	6860	6300
60	1.83×10^4	1.88×10^4

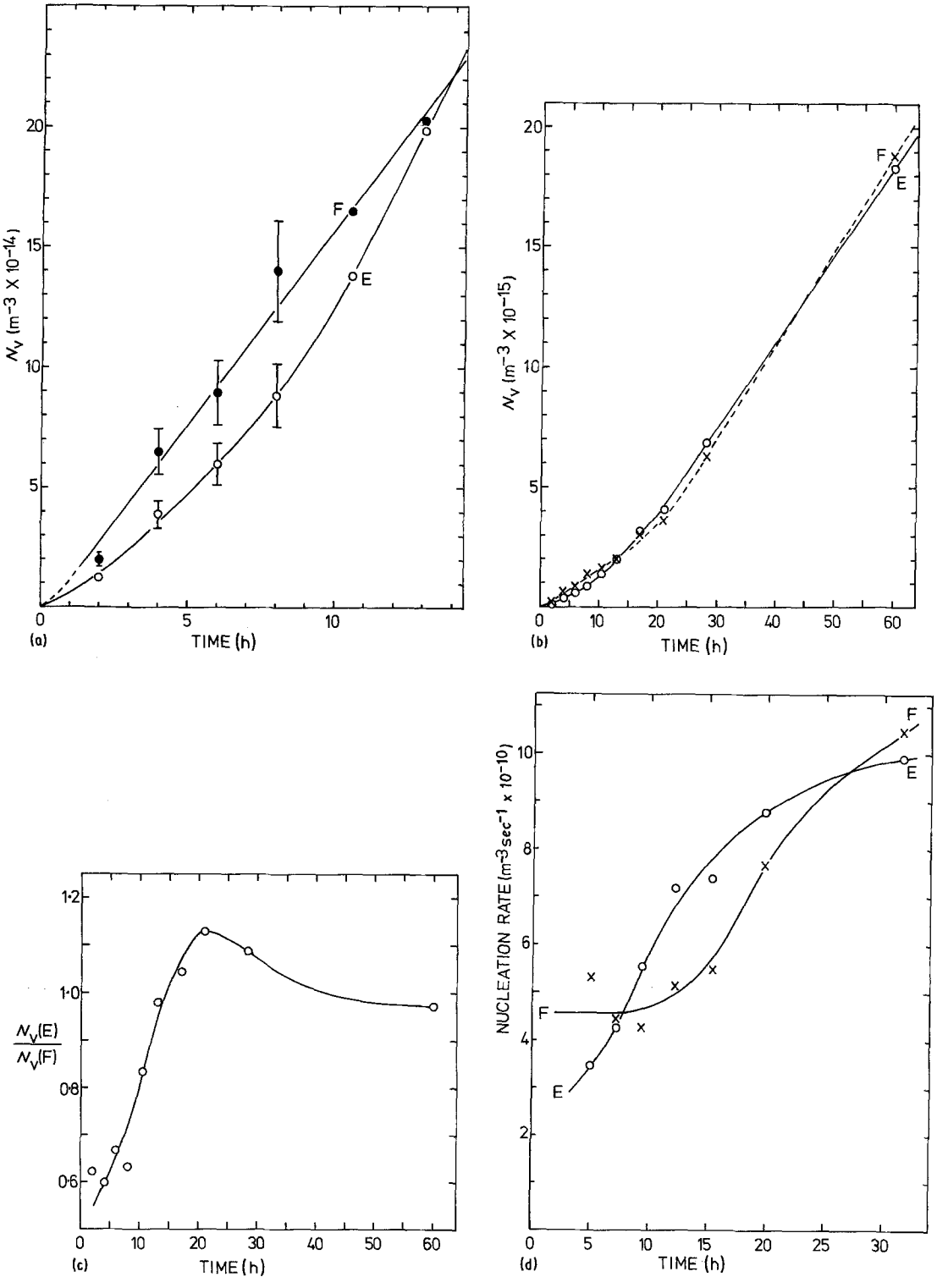

Figure 9 (a) and (b) Crystal nucleation kinetics in glass 28.5 at 700° C. N_v against time plots after prior heat treatments E and F (see text). Early stages shown in (a) and later stages in (b). In (a) points ○ (glass E), points ● (glass F). In (b) points ○ (glass E), points × (glass F). 95% confidence limits ±15% of values (marked ⊢——⊣).

(c) Ratio of N_v in glass E to N_v in glass F against time at 700° C.

(d) Crystal nucleation rates against time for glasses 28.5E and 28.5F determined from N_v against time plots in Figs. 9a and b using method described in text. Points ○ (glass E), points × (glass F). For glass F full line for times < 8 h is average nucleation rate over first six points.

differences between E and F were maintained from 17 to about 30 h. At longer times than this the glasses had identical values of N_v (and nucleation rates) to within experimental error.

The explanation of these results follows closely the arguments used for glass 25.3 in Section 3.2. No amorphous phase separation was detected in the as-cooled glass 28.5 (glass E) before heat treatment at 700° C. Thus the composition of this glass was initially further away from the $BaO \cdot 2SiO_2$ composition than the composition of the baria-rich matrix in the prior phase-separated glass F. Hence the crystal nucleation rate in F was initially higher than in E. However, the primary phase separation in E occurred more rapidly than the secondary phase separation in F due to the greater driving force in E. Also, the larger number of amorphous droplets nucleated in E at 700° C provided many more sites for diffusion controlled growth of droplets in this glass. Consequently the matrix composition in E shifted more rapidly than in F, becoming progressively richer in baria. Hence the crystal nucleation rate in E began to overtake that in F. After about 8 h the matrix composition in E became richer in baria than in F and the crystal nucleation rate in E became greater than in F. After about 14 h a "cross-over" in the N_v values occurred. Thereafter, as the matrix phases in both E and F approached their equilibrium values at 700° C the crystal nucleation rates became almost identical.

The crystal nucleation rate for glass F was nearly constant for the first 12 h, indicating that the composition of the baria-rich phase changed only slightly during this period. From 12 to 30 h the nucleation rate increased rapidly. This coincided with the major change in matrix composition, which occurred at a later stage than in glass E.

As in the case of glass 25.3 interfacial effects did not appear to influence the nucleation kinetics. For example, the number of crystals nucleated in E and in F at 700° C were very similar for nucleation times of 21 to 60 h, yet the phase separation morphologies of the glasses were very different. Thus the number of droplets in E was more than 10 times greater than in F and the interfacial area S_v in E was about 5 times greater than in F.

4. Conclusions

Isothermal experiments at 700° C on $BaO–SiO_2$ glasses containing 25.3 and 28.5 mol% BaO demonstrated that amorphous phase separation had a pronounced influence on the rates of crystal nucleation in these compositions. Thus marked differences in crystal nucleation occurred at 700° C, depending on the nature of the preliminary heat treatment given to each glass; for example, whether the glass had been heated at a higher temperature to induce phase separation or whether it had been rapidly quenched to suppress phase separation. Phase separation also occurred simultaneously with the crystal nucleation at 700° C, producing an increase in crystal nucleation rate with time, which was reflected in curved plots of N_v against time. As far as the authors are aware this is the first time this phenomenon has been clearly demonstrated in a glass system. In contrast, glass 30.4, which did not undergo amorphous phase separation, exhibited a linear N_v against time plot in accordance with the usual behaviour in non-phase separating glasses [9].

All the observed effects of phase separation on crystal nucleation could be clearly explained in terms of the composition of the baria-rich matrix phase. The average baria content of this phase increased gradually during the precipitation of the silica-rich droplets, approaching the equilibrium value given by the phase boundary. Also, from the results of Part 1 the crystal nucleation rate at a given temperature increased with increase in BaO content, the highest rate being observed at the stoichiometric barium disilicate composition. Furthermore, the interfaces between the amorphous phases did not appear to affect the crystal nucleation rates significantly in the present experiments at 700° C. These conclusions reinforce those of Part 1 of the present paper.

The results provided clear evidence of the variation of crystal nucleation rates at 700° C with composition in this system. For example, with the quenched samples of glass 25.3 the baria-rich phase shifted in composition from approximately 25.3 to 31.1 mol% BaO during heat treatment at 700° C. At the same time the crystal nucleation rate increased by about 10 times (Fig. 5d). Similarly, when the baria-rich phase in glass 28.5 shifted from approximately 28,5 to 31.1 mol% BaO during heat treatment at 700° C the crystal nucleation rate increased by about 3 times (Fig. 9d).

The ways in which a shift in glass composition due to phase separation may influence crystal

nucleation rates were considered in detail in Part 1. The nucleation rate I at a temperature T is given by

$$I = A \exp [-(W^* + \Delta G_D)/kT]$$

where W^* and ΔG_D are the thermodynamic and kinetic free energy barriers respectively, and A is essentially a constant. For a given temperature a change in composition will probably alter W^* and ΔG_D.

The relative importance of these two quantities may be assessed from viscosity data, if it is assumed that the term $\exp(\Delta G_D/kT)$ is proportional to viscosity. This approach was used to interpret the effects of composition on nucleation rates in lithia-silica and soda-lime-silica glasses not exhibiting immiscibility [9–12]. For these glasses, in general significant changes in both the ΔG_D and W^* terms were needed to account for the results. An attempt to carry out a similar analysis in the $BaO–SiO_2$ system using viscosity data and crystal growth measurements at high undercoolings [13] will be described in Part 3 of this paper [14]. It will be demonstrated that, as expected, viscosities fall and growth rates rise with increase in baria content for the composition range studied in this work. The results will also indicate that a change in composition due to phase separation produces significant changes in both the ΔG_D and W^* terms for crystal nucleation. From the earlier discussion in Part 1 it is probable that the thermodynamic driving force ΔG makes an important contribution to the variation in W^* with composition at a given temperature.

Acknowledgements

Thanks are due to Mr R. Bacon for help with the electron microscopy. AHR was supported by an SERC studentship during the period of this work.

References

1. A. H. RAMSDEN and P. F. JAMES, *J, Mater. Sci.* **19** (1984) 1406.
2. R. T. DEHOFF and F. N. RHINES, "Quantitative Microscopy" (McGraw-Hill, New York, 1968).
3. C. S. SMITH and L. GUTTMAN, *J. Met. Trans. AIME* **197** (1953) 81.
4. D. G. BURNETT and R. W. DOUGLAS, *Phys. Chem. Glasses* **11** (1970) 125.
5. A. H. RAMSDEN, PhD thesis, University of Sheffield, Sheffield, UK (1977).
6. T. P. SEWARD III, D. R. UHLMANN and D. TURNBULL, *J. Amer, Ceram. Soc.* **51** (1968) 278, 634.
7. W. HALLER, D. H. BLACKBURN and J. H. SIMMONS, *ibid.* **57** (1974) 120.
8. P. F. JAMES, *J. Mater. Sci.* **10** (1975) 1802.
9. *Idem*, in "Nucleation and Crystallization in Glasses", Advances in Ceramics Vol. 4, edited by J. H. Simmons, D. R. Uhlmann and G. H. Beall (The American Ceramic Society, Inc., Columbus, Ohio, 1982) pp. 1–48.
10. C. J. R. GONZALEZ-OLIVER, P. S. JOHNSON and P. F. JAMES, *J. Mater. Sci.* **14** (1979) 1159.
11. C. J. R. GONZALEZ-OLIVER, PhD thesis, University of Sheffield, Sheffield, UK (1979).
12. C. J. R. GONZALEZ-OLIVER and P. F. JAMES, XIII International Glass Congress, Hamburg, 1983, Poster Presentation.
13. E. D. ZANOTTO, PhD thesis, University of Sheffield, Sheffield, UK (1982).
14. E. D. ZANOTTO, A. F. CRAIEVICH and P. F. JAMES, *J. Mater. Sci.* to be published.

Received 24 October
and accepted 3 November 1983